Interaction of mono-carboxylic acids in benzene studied by small-angle neutron scattering

Viktor I. Petrenko [a,b,*], Mikhail V. Avdeev [a,c], László Almásy [d,e], Leonid A. Bulavin [b], Victor L. Aksenov [c,a], László Rosta [f], Vasil M. Garamus [g]

[a] Frank Laboratory of Neutron Physics, Joint Institute for Nuclear Research, Dubna, Russia
[b] Physics Department, Kyiv Taras Shevchenko National University, Kyiv, Ukraine
[c] Russian Research Center "Kurchatov Institute", Moscow, Russia
[d] Adolphe Merkle Institute, University of Fribourg, CH-1700 Fribourg, Switzerland
[e] Laboratory for Neutron Scattering, PSI and ETH Zürich, CH-5232 Villigen, Switzerland
[f] Research Institute for Solid State Physics and Optics, Hungarian Academy of Sciences, Budapest, Hungary
[g] GKSS Research Centre, Geesthacht, Germany

The intermolecular interaction of non-saturated (oleic acid) and saturated (stearic and myristic acids) mono-carboxylic acids in a non-polar organic solvent (deuterated benzene) is derived from the concentration dependence of the small-angle neutron scattering. The excluded volume repulsion dominates over the attraction (supposed due to van der Waals forces) for oleic and myristic acids. In turn, for stearic acid the attractive component is higher than the repulsive one; this results in a shift of the transition into the liquid crystalline state (because of molecule anisotropy) towards smaller concentrations and could explain early data on worse stabilization properties of stearic acid in ferrofluids compared to oleic and myristic acids.

1. Introduction

Oleic acid (OA) $(CH_3(CH_2)_7CH=CH(CH_2)_7COOH)$, a non-saturated mono-carboxylic acid, is a classical stabilizing agent used in the synthesis of ferrofluids for coating magnetic nanoparticles in non-polar organic liquids [1]. The reason for high stabilization efficiency of oleic acid is often associated with its non-saturated bond, which results in a kink ($\approx 120°$ [2]) in the middle of the molecule. This conclusion comes from the fact that the strictly linear saturated analog of oleic acid, stearic acid (SA) $(CH_3(CH_2)_{16}COOH)$, exhibits extremely low stabilization efficiency in ferrofluids. This difference is not fully understood, and, after more than thirty years (first ferrofluids appeared in the middle of 1960s), still the problem is referred to as a "puzzle of stearic acid" [3]. Based on measurements of wettability of surfactant layers between mica surfaces by hexadecane, Tadmor et al. explained [3] this difference by better solvation of oleic acid. It was claimed that it is the kink

in the oleic surfactant tails that weakens their nematic attraction and thus favors their solvation.

After Shen et al. [4] who probed short chain length mono-carboxylic acids in the stabilization of water-based ferrofluids, it was recently shown [5] that myristic acid (MA) $(CH_3(CH_2)_{12}COOH)$ and lauric acid $(CH_3(CH_2)_{10}COOH)$ reveal better possibility for stabilizing magnetite in non-polar organic liquids as compared to stearic acid. However, the size and dispersity of magnetic particles stabilized by myristic and lauric acids are significantly smaller than in the case of stabilization by oleic acid, while the effective thickness of the surfactant layer is approximately the same. Thus, the efficiency of stabilization of mono-carboxylic acids was related [5] to repulsion properties of the surfactant layer around magnetite, which determine the stable size distribution of magnetic particles in ferrofluids. If oleic acid is proved to be highly efficient surfactant to stabilize nanomagnetite over the wide interval of radii of 1–10 nm (result of condensation reaction), myristic and lauric acids stabilize partially this interval dispersing in the carrier only a fraction of smaller particles.

In the present paper we show that an important contribution into the difference in the stabilizing properties of non-saturated oleic acid and saturated acids can come from van der Waals interaction between molecules in bulk solutions. We suppose that this

---

* Corresponding author at: Frank Laboratory of Neutron Physics, Joint Institute for Nuclear Research, Joliot-Curie 6, 141980 Dubna, Moscow Reg., Russia. Tel.: +7 496 21 65 444; fax: +7 496 21 65 484.
E-mail address: vip@nf.jinr.ru (V.I. Petrenko).

interaction also affects strongly the transition into the nematic phase in concentrated solutions of saturated mono-carboxylic acids. Here, we compare the behavior of OA, SA and MA in pure deuterated benzene (d-benzene) using data of small-angle neutron scattering (SANS). The deuterated solvent is chosen to get better signal (coherent scattering from the molecules) to noise (incoherent contribution coming mainly from hydrogen) ratio. The concentration dependences of integral parameters of the scattering curves (forward scattered intensity and radius of gyration) are used to conclude about the character of interaction of the studied molecules in solutions. The characteristic size of the acid molecules (2 nm) is close to the resolution limit of the SANS method. This means that, in contrast to longer rod-like molecules, where the structure- and form-factors are modeled over the experimentally accessible momentum transfer range [e.g. 6–8], in the present case only the Guinier region of the scattering curves can be reliably treated. As it is known, for rod-like particles (anisotropic particles) the excluded volume interaction consists of isotropic and orientation dependent (nematic attraction) terms. The important feature of the treatment below is that the forward scattering as a function of the solute concentration depends only on the isotropic part of the intermolecular interaction [9]. This makes it possible to analyze the isotropic part of the interaction in the system of strongly anisotropic particles. The results are discussed with respect to potential reasons of different stabilization properties of mono-carboxylic acids in ferrofluids.

2. Experimental

Pure oleic (98%), stearic and myristic (both 99.9%) acids (Merck) were dissolved in d-benzene, C_6D_6 (100%, Sigma–Aldrich) with ultrasonication. Several solutions within intervals of 5–35% (OA), 3–25% (MA) and 2–7% (SA) in volume fraction were studied. The choice of such intervals was determined, on the one hand, by the sensitivity of the used SANS method (lower limit), and, on the other hand, by acid solubility in benzene (upper limit). An increase in the concentration of MA and SA towards higher values than indicated above results in vigorous growth of viscosity followed by the formation of new jelly-like phase, which we connect with the transition into the liquid crystalline state well-known in thermodynamics of stiff rod-like polymers [6,9–16].

SANS experiments were performed on the YuMO small-angle time-of-flight diffractometer at the IBR-2 pulsed reactor, Joint Institute for Nuclear Research, Dubna, Russia and the Yellow Submarine small-angle instrument at the steady-state reactor of the Budapest Neutron Centre (BNC), Hungary. The differential cross-section per sample volume (called hereafter scattered intensity) was obtained as a function of the momentum transfer module, $q = (4\pi/\lambda)\sin(\theta/2)$, where λ is the incident neutron wavelength and θ is the scattering angle, over the q-interval of 0.2–4 nm^{-1}. The raw data treatment was performed as described elsewhere [17].

For monodisperse nonspherical particles in a homogeneous solvent the scattered intensity can be written using the decoupling approximation [18,7]:

$$I(q) = \frac{\Phi}{V}(b_{tot} - \rho_s V)^2 \left\langle \left| F(q) \right|^2 \right\rangle S'(q), \qquad (1)$$

where Φ is the volume fraction of the solute; V is the volume of a single solute particle; $b_{tot} = \Sigma b_i$ is the sum of coherent scattering lengths; b_i, taken over a particle; ρ_s is the solvent scattering length density; $\langle |F(q)|^2 \rangle$ is the squared form-factor of a single particle averaged over the particle orientations (defined in a way that $F(0) = 1$); $S'(q) = 1 + \beta(q)[S(q) - 1]$, where $S(q)$ is the structure-factor calculated for the average particle size and reflecting the interference of scattering from different particles, thus, comprising information about the interaction in the solution, and $\beta(q) = |\langle F(q)\rangle|^2/\langle |F(q)|^2 \rangle$ is a q-dependent anisotropy factor. $S(q)$ is related

to the pair radial distribution function, $g(r)$, in the way:

$$S(q) = 1 + \frac{4\pi\Phi}{V} \int_0^\infty (g(r) - 1)\frac{\sin(qr)}{qr}r^2 dr, \qquad (2)$$

where r is the distance between particles centers of mass.

At sufficiently small q-values, scattered intensity can be described by the Guinier approximation:

$$I(q) = I(0) \exp\left(-\frac{(qR_g)^2}{3}\right) \qquad (3)$$

with two parameters, which are the forward scattered intensity, $I(0)$, and the apparent radius of gyration, R_g. Their change with the solute concentration reflects the effective interaction between particles. Despite high anisotropy ratio of the considered molecules (between 6 and 8), the $\beta(q)$ function differs slightly from unity in the Guinier region ($qR_g < 1$), so $S'(q) \approx S(q)$. At $q = 0$ one can exactly write $S'(0) = S(0)$. When fitting the curves, the residual experimental background was varied as an additional term in (3). Following Refs. [19–21] the effects of the finite angular resolution and the wavelength spread were estimated to be negligibly small (<0.01%) for the derived values of the radius of gyration and forward scattered intensity and were not taken into account.

The obtained dependences $S(0)$ on the volume fraction of solutes was compared with theoretical calculations for solution of straight stiff rod-like particles according to [10,11] and [9] (random phase approximation model), as well as for the case of hard sphere interaction [22,23].

3. Results

The Guinier plots of the experimental SANS curves for OA and MA at different volume fractions, Φ, of the solute are presented in Fig. 1. The obtained residual background is subtracted from the curves. The data are well approximated by the Guinier approximation (3). In the insets the scattering curves normalized to the volume fraction of the solute, $I/\Phi \sim q$, are presented in double logarithmic plot. The curves approach each other at large q-values, indicating their consistency in respect to the used volume fractions, as well as to the subtracted background.

In both OA and MA systems the concentration dependences of the forward scattered intensity and the apparent radius of gyration (Fig. 2) show a linear behavior within the whole concentration range covered. It can be approximated by a function:

$$\frac{I(0)}{\Phi} = CS(0) \approx C(1 + B\Phi), \qquad (4)$$

where $C = (b_{tot} - \rho_s V)^2/V$; B plays the role of the dimensionless second virial coefficient [24–28], which can be expressed via the pair radial distribution function as

$$B = \frac{1}{V} \int [g(r) - 1]dV. \qquad (5)$$

The sign of this coefficient corresponds to the repulsive ($B < 0$) or attractive ($B > 0$) type of interaction in the solution. Thus, for the hard sphere interaction $B = -8$. In this approximation for the concentration dependence of the apparent radius of gyration one can write [25]:

$$R_g^2 \sim R_{g0}^2 + \frac{\Phi BP^2}{1 + \Phi B} \approx R_{g0}^2 + \Phi BP^2, \qquad (6)$$

where R_{g0} is the real radius of gyration of the particle, and P is some parameter related to the $g(r)$ function. The given notation results in the same character in the change of $I(0)/\Phi$ and R_g^2 with respect to the sign of B. The values of B coefficient and R_{g0} found by (4) and (6), respectively, are given in Table 1. The experimental
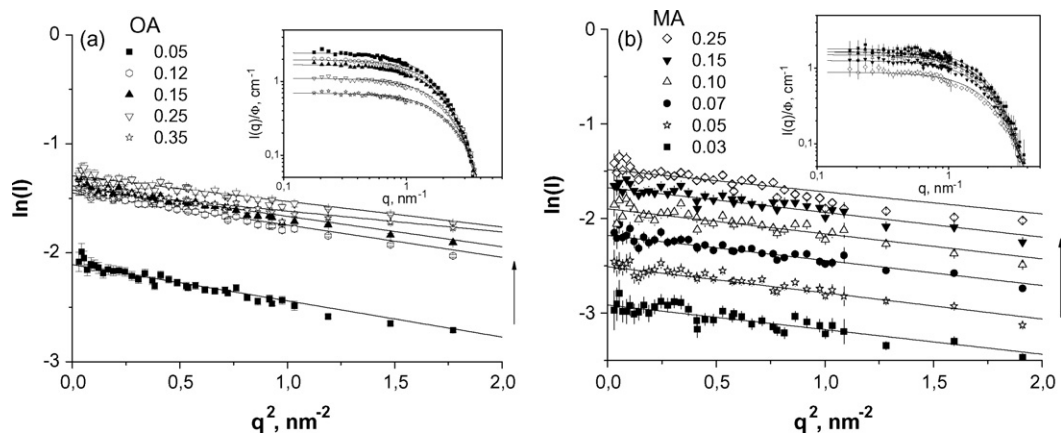
Fig. 1. Guinier plots of experimental SANS curves from solutions of OA (a) and MA (b) in d-benzene. The curves are shown in absolute scale. Arrows indicate the concentration growth. Insets show scattering normalized to the volume fraction of solute in the double logarithmic scale. Solid lines in all graphs correspond to Guinier approximations.

Table 1
Parameters derived from the SANS data and their comparison with the calculated values.

Acid	B	V_{excl} (Å^3)	V_{exp} (Å^3)	V_{exp}/V_{excl}	L (Å)	R (Å)	$R_{g0,calc}$ (Å)	R_{g0} (Å)
OA	-2.2 ± 0.1	540	669 ± 50	1.23 ± 0.09	23	3.0 ± 0.2	6.4	11.0 ± 0.3
SA	$+4 \pm 1$	540	644 ± 80	1.19 ± 0.15	23	3.0 ± 0.4	6.9	9 ± 1
MA	-2.0 ± 0.1	432	522 ± 50	1.2 ± 0.1	18	3.0 ± 0.3	5.6	9.3 ± 0.1

B: dimensionless second virial coefficient from linear fit of (4); V_{excl}: excluded volume of acids molecules estimated by Tanford's formula [29]; V_{exp}: experimental molecular volume of the acids in solution from linear fit of (4); L: molecule length calculated by Tanford's formula [29]; R: cross-section radius from equation $V_{exp} = \pi R^2 L$; $R_{g0,calc}$: calculated radius of gyration for single acid molecules; R_{g0}: experimental value of apparent radius of gyration extrapolated to zero concentration from linear fit to (6).

molecular volumes of the acids molecules in solution (V_{exp}) were calculated from the constant C in (4). In Table 1 they are compared with excluded volumes (V_{excl}) estimated by Tanford's formula [29]. Also, the Tanford's length [29], L, was used for estimating the cross-section radius of the molecules, R, from equation $V_{exp} = \pi R^2 L$. With the obtained values of L and R the radii of gyration for single acid molecules, $R_{g,calc}$, were calculated according to well-known formulas [30] for straight and bent cylinders. Parameters L, R, $R_{g,calc}$ are given in Table 1.

Negative slopes in Fig. 2 corresponding to (4) and (6) for OA and MA systems indicate the total repulsive character of the interaction in these solutions. Along with it, a significant attractive component is present. Indeed, for straight MA the experimental dependence $I(0)/\Phi \sim \Phi$ differs from the predictions of various theoretical models (Fig. 2a). The closest to the experimental data is the case of the random phase approximation (RPA) model for the straight

rigid rod-like particles [9]. This model considers in a standard way [31–33,9] the excluded volume interaction between such particles as a sum of isotropic and orientation dependent contributions. Below, the second contribution is referred as nematic attraction. As it was mentioned in Introduction, despite the additional orientation dependent interaction, the concentration dependence of $S(0)$ is determined only by the isotropic excluded volume interaction [9]:

$$\frac{I(0)}{\Phi} = CS(0) = \frac{C}{1 + nLv_0} \approx C(1 - nLv_0) = C\left(1 - \frac{L}{R}\Phi\right), \qquad (7)$$

where $v_0 = \pi RL$ is the parameter of the isotropic excluded volume potential; n is the particle number density; and $B = -L/R$ is determined by the asymmetry of the molecules. For MA one can find $B = -L/R = -6$ (using data in Table 1). Thus, the additional "isotropic" attraction besides the excluded volume interaction can be con-
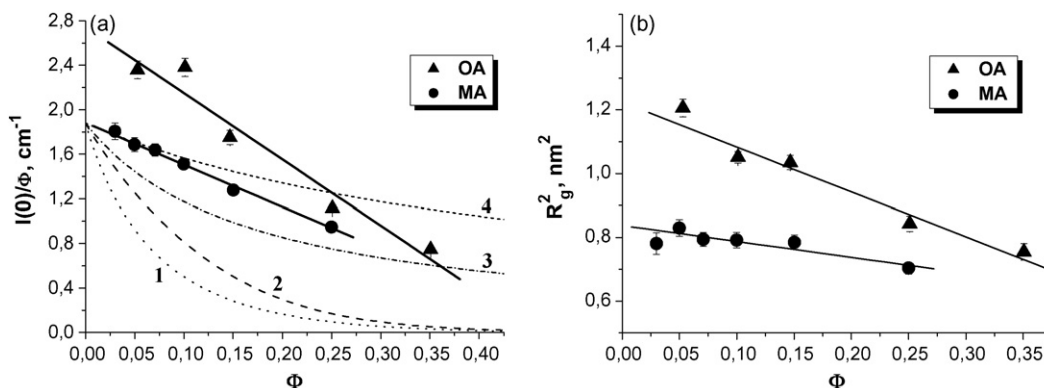

Fig. 2. Forward scattered intensity referred to one volume fraction of solute (a) and squared radius of gyration (b) vs. acid volume fraction for solutions of oleic and myristic acids in d-benzene. Solid lines show linear fits in accordance with (4) and (6), respectively. The following theoretical calculations for MA are given in (a): 1: according to scaled particle approach for fluids of rigid spherocylinders and through consideration of reversible work necessary to add a scaled spherocylinder at arbitrary fixed point in the fluid [10,11]; 2: hard sphere potential [22,23]; 3: according to RPA model for the straight rigid rod-like particles [9] with $v_0 = \pi RL = 170\,\text{Å}^2$; 4: according to [9] but with reduced $v_0 = \pi R^2(-4.0 + L/R) = 57\,\text{Å}^2$.
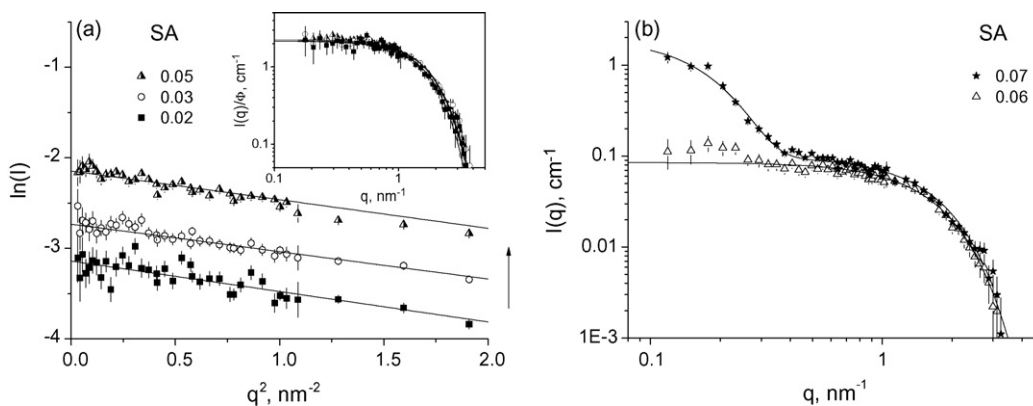
3

Fig. 3. Experimental SANS curves from solutions of stearic acid (SA) in d-benzene with various volume fractions of the acid. (a) Guinier plots of experimental SANS curves for the Φ-interval of 0.02–0.05 in absolute scale. Arrow indicates the concentration growth. Inset shows the scattered intensity normalized to the volume fraction of solute in the double logarithmic scale. Solid lines in both graphs correspond to Guinier approximations. (b) Scattered intensity for $\Phi > 0.05$ in absolute scale. Solid lines correspond to Guinier approximations. For $\Phi = 0.06$ the fitted apparent radius of gyration $R_g = 1.1$ nm; for $\Phi = 0.07$ two Guinier-type terms give $R_g = 1.1$ nm (large q-values) and $R_g = 5.8$ nm (small q-values).

cluded. The theoretical curve $I(0)/\Phi \sim \Phi$ can be forced to be much closer to the experimental data by decreasing the ν_0 parameter (Fig. 2a) to fit experimental B value, this would correspond to a decrease in the repulsion. For OA we cannot use (7) because of its kinked shape. Nevertheless, one can note that the effective asymmetry of the OA molecule is quite close to that of MA. Indeed, neglecting the molecule shape and considering OA as an cylinder with the same volume and radius of gyration one obtains for such cylinder $L = 20.7$ Å, $R = 3.2$ Å, which gives $L/R \approx 6.5$. Thus, approximately the same "isotropic" attraction as in the MA case should contribute to interaction between OA. For the moment we find this feature to be the only one, which can be connected to the fact that OA and MA show similar interaction behavior in solutions.

The behavior of the scattering curves for SA solutions (Fig. 3) is drastically different compared to the OA and MA solutions. In the concentration range of $\Phi = 0.02$–0.05, in contrast to the previous case, the Guinier approximation (Fig. 3a) reveals an increase both in normalized forward scattered intensity and in the apparent radius of gyration with the growth of the acid concentration (Fig. 4). All parameters (Table 1) were estimated in the same way by (4) and (6) using three points in the denoted interval. The positive sign of B for SA solutions indicates effective attraction between acid molecules. Above $\Phi = 0.05$ this attraction results in partial aggregation, which is reflected in a deviation of the data from the Guinier law at the

smallest q-values (Fig. 3b). At $\Phi = 0.07$ the SANS signal from these aggregates is rather distinguished, their characteristic size can be roughly estimated from an additional Guinier-type term in (3) as ~ 10 nm.

4. Discussion

The presented results indicate that OA and MA molecules show quite similar behavior in benzene in terms of the interaction. Besides the dominating excluded volume repulsion, an attractive component is seen in the pair interaction potential. As mentioned above, this component is not connected with the nematic attraction, since it is obtained from the analysis of $S(0)$. Attraction becomes strong enough in the SA solution to be the major contribution, which provides in total the effective attraction between the acid molecules. So, we can assume that this attraction is responsible for different stabilization properties of acids at the synthesis of ferrofluids in addition to the better solvatation of OA, discovered by Tadmor et al. [3]. Such assumption is supported by experimental facts that OA and MA are quite good surfactants for ferrofluids and SA is worse.

The effect of the nematic attraction can be seen only for the concentration dependence of R_g. One can see a difference (Table 1) in radii of gyration calculated for single molecules and those found in the solution at the smallest concentrations, which is a result of the nematic interaction effect. Indeed, such interaction affects the $S(q)$ expansion at small q-values through an additional term Dq^4 with the concentration dependent parameter D [9]. For the considered Φ-interval D is positive, so the term Dq^4 makes larger the apparent radius of gyration of the Guinier approximation.

One can assume that the observed attraction is mainly a result of the dispersion forces (van der Waals interaction). It increases with the molecular size, which can explain why the behavior of bent OA and straight MA are close to each other and differs from that of SA. An important factor can be also the solute–solvent interaction connected with a special arrangement of benzene molecules on the acid surface (solvation), as the size of the solvent molecule is comparable with that of the solutes. The experimental volumes obtained by SANS are larger than the calculated excluded volumes, indicating the presence of a solvation shell at the molecular surface. However, the ratio V_{exp}/V_{excl} is approximately the same for all acid molecules (Table 1), hence, solvation cannot explain the difference in the attraction of the molecules.

The interesting question is the role of the observed attraction in the transition into the nematic phase in these solutions. As it was
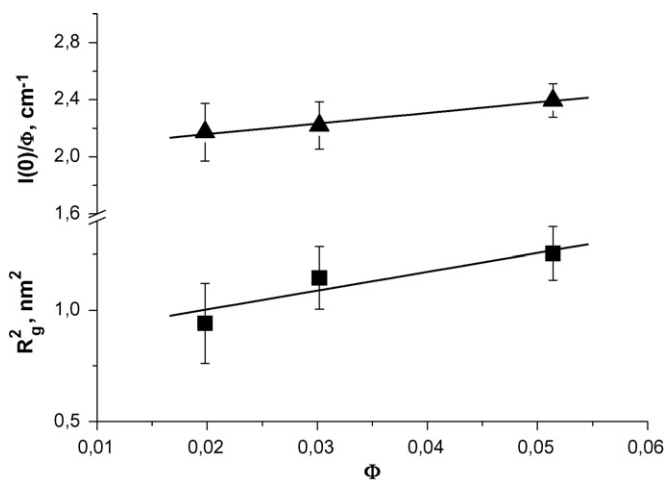

Fig. 4. Forward scattered intensity normalized to concentration (triangle) and apparent radius of gyration (square) vs. SA volume fraction in d-benzene. Solid lines show linear fits in accordance with (4) and (6), respectively.

mentioned above, this transition starts at $\Phi > 0.05$ in the SA solution and at $\Phi > 0.25$ in the MA solution. For straight rigid cylinders with only nematic attraction the critical concentration is inversely proportional to the molecule length [9]. One can see that this is not the case for strictly linear MA and SA molecules. The inverse ratio of MA and SA lengths, 1.3, is significantly smaller than the ratio of the observed critical concentrations, ≈ 4. We suppose that the van der Waals attraction shifts the transition into the liquid crystalline phase towards smaller acid concentrations. It is also supported by the comparison of the experimental critical concentrations with theoretical predictions, which take into account only the excluded volume interaction [10,11]. For SA and MA these estimates give values of 0.24 and 0.29, respectively, so the lowering of the critical concentration for SA is rather significant. Formation of aggregates detected in the SA solutions above $\Phi = 0.05$ should be related with the discussed transition. They could be small domains of nematic aggregates, rather than inverse micelles, since the observed aggregates are definitely larger than a micelle having radius of about the molecular length (≈ 2 nm). The character of the curve (Fig. 3b) reflects clearly that only a part of acids molecules are within the aggregates. However, it is difficult to estimate the number density of aggregates from the forward scattering, since the knowledge of the aggregate shape (at least, its anisotropy) is required. Similar aggregation behavior of stearic acid as a result of the liquid crystalline like packing of the alkyl tails was observed also in aqueous solutions [34].

The formation of the nematic phase in bulk solutions of monocarboxylic acids is an important factor in the stabilization procedure of magnetic fluids. In the standard procedure, pure solutions of these acids are added to aqueous solutions where the nanomagnetite forms. The principle of the stabilization method is based on the chemisorption of the acid heads on the magnetite surface. It is obvious that formation of acid aggregates would hinder this process. The fact that the nematic transition in the SA case is significantly shifted to small concentrations because of the strong van der Waals attraction should be considered further with respect to poor stabilizing properties of SA in ferrofluids.

5. Conclusion

Comparing the behavior of saturated and non-saturated monocarboxylic acids in a non-polar solvent, benzene, we found that interactions of MA and OA in solutions are repulsive, while interactions between SA molecules are attractive (most likely due to van der Waals forces) affecting the transition into the liquid crystalline state.

References

[1] R.E. Rosensweig, Ferrohydrodynamics, Cambridge University Press, Cambridge, 1985.
[2] S. Abrahamson, I. Ryderstedt-Nahringbaur, The crystal structure of the low-melting form of oleic acid, Acta Crystallogr. 15 (1962) 1261.
[3] R. Tadmor, R.E. Rosensweig, J. Frey, J. Klein, Resolving the puzzle of ferrofluid dispersants, Langmuir 16 (2000) 9117.
[4] L. Shen, P.E. Laibinis, T.A. Hatton, Bilayer surfactant stabilized magnetic fluids: synthesis and interactions at interfaces, Langmuir 15 (1999) 447.
[5] M.V. Avdeev, D. Bica, L. Vékás, et al., On the possibility of using short chain length mono-carboxylic acids for stabilization of magnetic fluids, J. Magn. Magn. Mater. 311 (2007) 6.
[6] N.J. Wagner, L.M. Walker, Structure of isotropic solutions of rigid macro-molecules via small-angle neutron scattering: poly(gamma-benzyl L-glutamate)/deuterated dimethylformamide, Macromolecules 28 (1995) 5075.
[7] J. Kalus, H. Hoffmann, K. Ibel, Small-angle neutron scattering on shear-induced micellar structures, Colloid Polym. Sci. 267 (1989) 818.
[8] P.G. Cummins, E. Staples, J.B. Hayter, J. Penfold, A small-angle neutron scattering investigation of rod-like micelles aligned by shear flow, J. Chem. Soc., Faraday Trans. 1 (83) (1987) 2773.
[9] T. Shimada, M. Doi, K. Okano, Concentration fluctuation of stiff polymers. I. Static structure factor, J. Chem. Phys. 88 (1988) 2815.
[10] M.A. Cotter, D.E. Martire, Statistical mechanics of rodlike particles. I. A scaled particle treatment of a fluid of perfectly aligned rigid cylinders, J. Chem. Phys. 52 (1970) 1902.
[11] M.A. Cotter, D.E. Martire, Statistical mechanics of rodlike particles. II. A scaled particles investigation of the aligned-isotropic transition in a fluid of rigid spherocylinders, J. Chem. Phys. 52 (1970) 1909.
[12] J.D. Parsons, Nematic ordering in a system of rods, Phys. Rev. A 19 (1979) 1225.
[13] M.A. Corter, Hard-rod fluid: scaled particle theory revisited, Phys. Rev. A 10 (1974) 625.
[14] L.M. DeLong, P.S. Russo, Thermodynamic and dynamic behavior of semiflexible polymers in the isotropic phase, Macromolecules 24 (1991) 6139.
[15] P. Padilla, E. Velasco, The isotropic–nematic transition for the hard Gaussian overlap fluid: testing the decoupling approximation, J. Chem. Phys. 106 (1997) 10299.
[16] M. Surve, V. Pryamitsyn, V. Ganesan, Dispersion and percolation transitions of nanorods in polymer solutions, Macromolecules 40 (2007) 344.
[17] M.V. Avdeev, A.A. Khokhryakov, T.V. Tropin, et al., Structural features of molecular-colloidal solutions of C60 fullerenes in water by small-angle neutron scattering, Langmuir 20 (2004) 4363.
[18] M. Kotlarchyk, S.H. Chen, Analysis of small angle neutron scattering spectra from polydisperse interacting colloids, J. Chem. Phys. 79 (1983) 2461.
[19] T. Freltoft, J.K. Kjems, Power-law correlations and finite-size effects in silica particle aggregates studied by small-angle neutron scattering, Phys. Rev. B 33 (1986) 269.
[20] J.S. Pedersen, D. Posselt, K. Mortensen, Analytical treatment of the resolution function for small-angle scattering, J. Appl. Crystallogr. 23 (1990) 321.
[21] E.P. Kozlova, Yu.M. Ostanevich, L. Cser, Main features of axially symmetric geometry of small angle scattering, Nucl. Instrum. Methods 169 (1980) 597.
[22] D.J. Kinning, E.L. Thomas, Hard-sphere interactions between spherical domains in diblock copolymers, Macromolecules 17 (1984) 1712.
[23] J.S. Pedersen, Analysis of small-angle scattering data from polymeric and colloidal systems: modelling and least-squares fitting, Adv. Colloid Interface Sci. 70 (1997) 171.
[24] F. Bonneté, D. Vivarès, Interest of the normalized second virial coefficient and interaction potentials for crystallizing large macromolecules, Acta Crystallogr. D 58 (2002) 1571.
[25] V.Yu. Bezzabotnov, L. Cser, T. Grosz, et al., Small-angle neutron scattering in aqueous solutions of tetramethylurea, J. Phys. Chem. 96 (1992) 976.
[26] G. Jancsó, L. Cser, T. Grósz, Yu.M. Ostanevich, Hydrophobic interactions and small-angle neutron scattering in aqueous solutions, Pure Appl. Chem. 66 (1994) 515.
[27] N.K. Székely, G. Jancsó, Small-angle neutron scattering and volumetric studies of dilute solutions of N,N′-dimethylpropyleneurea in heavy water, J. Phys. Chem. A, doi:10.1021/jp808471p, in press.
[28] N.K. Székely, L. Almásy, G. Jancsó, Small-angle neutron scattering and volumetric studies of dilute solutions of N,N′-dimethylethyleneurea in heavy water, J. Mol. Liq. 136 (2007) 184.
[29] C. Tanford, Micelle shape and size, J. Phys. Chem. 76 (1972) 3020.
[30] L.A. Feigin, D.I. Svergun, Structure Analysis by Small-angle X-ray and Neutron Scattering, Plenum Press, NY, 1987.
[31] F. Jahnig, Molecular theory of lipid membrane order, J. Chem. Phys. 70 (1979) 3279.
[32] A. ten Bosch, P. Maissa, P. Sixou, Molecular model for nematic polymers in liquid crystal solvents, J. Chem. Phys. 79 (1983) 3462.
[33] A. ten Bosch, P. Sixou, Screening in semirigid polymer systems, J. Chem. Phys. 83 (1985) 899.
[34] J.R. Kanicky, D.O. Shah, Effect of degree, type, and position of unsaturation on the pK_a of long-chain fatty acids, J. Colloid Interface Sci. 256 (2002) 201.